IEEE Access
Multidisciplinary | Rapid Review | Open Access Journal

Received August 29, 2018, accepted September 20, 2018, date of publication October 1, 2018,
date of current version December 7, 2018.

Digital Object Identifier 10.1109/ACCESS.2018.2872572

Improved Multi-Step Look-Ahead Control Policies for Automated Manufacturing Systems

CHAO GU[1], ZHIWU LI[1,2], (Fellow, IEEE), NAIQI WU[2,3], (Senior Member, IEEE), MOHAMED KHALGUI[4], TING QU[4], AND ABDULRAHMAN AL-AHMARI[5]

[1]School of Electro-Mechanical Engineering, Xidian University, Xi'an 710071, China
[2]Institute of Systems Engineering, Macau University of Science and Technology, Macau 519020, China
[3]The National Key Laboratory of Precise Electronic Manufacturing Technology and Equipment, Guangdong University of Technology, Guangzhou 510006, China
[4]School of Electrical and Information Engineering, Jinan University (Zhuhai Campus), Zhuhai 519070, China
[5]Industrial Engineering Department, King Saud University, Riyadh 12372, Saudi Arabia

Corresponding authors: Zhiwu Li (zhwli@xidian.edu.cn) and Naiqi Wu (nqwu@must.edu.mo)

This work was supported in part by the National Natural Science Foundation of China under Grants 61603285 and U1401240, and in part by the Science and Technology Development Fund (FDCT) under Grants 106/2016/A3 and 122/2017/A3.

ABSTRACT The deadlock control problem in automated manufacturing systems (AMSs) has received much attention in recent years due to the flexibility of an AMS. In the framework of Petri nets, resource-transition circuits and siphons are often used to characterize and derive a deadlock control policy for an AMS. This paper mainly focuses on a class of Petri nets, namely, the system of simple sequential processes with resources, which contains some special resource places. For such a class of Petri nets, the relationship between a multi-step look-ahead deadlock avoidance control method and the structure of the model is established and expanded in a mathematical way. Unlike the one-step look-ahead deadlock avoidance policy (DAP) proposed in the literature, the DAPs reported in this research are applicable to more complex situations, including a model with one-unit resource shared by two or more perfect resource-transition circuits that do not contain each other. Compared with the existing work, some results are archived for expanded models. Finally, for the model with two shared one-unit resources, specific solutions are also presented. Meanwhile, examples are used to demonstrate the proposed results.

INDEX TERMS Automated manufacturing system, Petri net, deadlock avoidance policy.

I. INTRODUCTION

MUCH attention in recent years has focused on the modeling and control of automated manufacturing systems (AMSs). An AMS consists of a finite set of resources, each of which is able to process multiple kinds of parts according to a specified sequence of operations. Generally, a great challenge of harnessing an AMS is to make its operation more efficient. Deadlocks are deemed as a fundamental and common issue in the management of an AMS, since their occurrence can disable the consecutive operation of an overall AMS. Consequently, it is generally recognized that the problem of deadlock avoidance or prevention should be effectively resolved.

As a widely used tool and profitable technology for discrete event systems [23], an important class of man-made systems that are usually computer-integrated [17]–[20], Petri nets are powerful for production system modeling [30], [35], scheduling and control [23], [25], [29], [32], [34], [35], [40]–[42], [44]–[46], [57]. To control an AMS is to restrict its behavior to satisfy the desired control specifications. By using Petri nets, a lot of work has been done to handle deadlock problems and there are mainly three types of methods: deadlock prevention, detection and recovery, and avoidance [2], [5]–[10], [15], [16], [33], [36], [38], [39]. Moreover, different Petri net classes are also developed for many other purpose [47].

Currently, the research on deadlock control is mainly based on structural analysis, such as siphons [27], [28], [52], [53] and resource-circuits or reachability graphs. The work in [8] reports a siphon-based deadlock control policy by exploring the fact that an unmarked siphon at a marking implies the occurrence of a deadlock state. A control place, sometimes called a monitor, is designed for each siphon such that the siphon cannot be emptied at any reachable marking. However, this method suffers from the structural complexity problem, since the number of control places is equal to that of siphons to be controlled. In 2004, Li and Zhou [14] put forward the concept of elementary siphons. They prove that deadlocks can be prevented by adding a control place for each elementary siphon to ensure that, under some conditions, all the siphons are marked at any reachable marking. This method requires less control places and thus is applicable to large-sized Petri nets. In order to avoid a complete siphon enumeration, the work in [43] develops a mixed integer programming (MIP)-based deadlock detection method that enumerates a portion of siphons only. A series of studies on a variety of deadlock control approaches with the Petri net formalism is reviewed and compared in [21] from the standpoint of structural complexity, behavior permissiveness, and computational complexity of designing a liveness-enforcing supervisor for an AMS.

Inspired by the work in [1], [16], and [9], this paper investigates the synthesis problem of a deadlock avoidance police (DAP), with polynomial-complexity, for AMSs in the framework of Petri nets. Deadlocks can be described by the maximal *perfect* resource-transition circuits (MPRT-circuits) that are saturated at a reachable state. As their name suggests, a resource-transition circuit in a Petri net modeling an AMS is a circuit consisting of resource places and transitions only. A resource is said to be a ξ-resource if its capacity is one and shared by two or more MPRT-circuits that do not contain each other. By using the deadlock characteristic description, it is first proved that there are only two types of reachable markings: deadlock and non-deadlock ones in an AMS modeled by an S^3PR without a ξ-resource [2]. Under this circumstance, a DAP needs to prohibit the transitions whose firing leads a system to deadlocks only. Consequently, an optimal DAP can be formulated by a one-step look-ahead policy [2], [3] to check whether the forthcoming state is deadlock or not. Furthermore, the proposed optimal DAP in [2] and [3] is of polynomial complexity with respect to the system scale. For an S^3PR containing ξ-resources, the work in [3] indicates that it is worthy to explore a multiple-step look-ahead policy such that its computation remains tractable.

This work is mainly devoted to this kind of problem. Enlightened by the work in [1]–[3], an optimal DAP for more general S^3PR with a ξ-resource is reported. The work in [1] mainly focuses on the DAP of a subclass of S^3PR with only one ξ-resource, namely the US^3PR. By introducing a conservative multiple-step look-ahead law, it is proved that the steps to look ahead in an optimal DAP merely depend on the structure of a US^3PR, which is the inherent nature of the model. Meanwhile, a multiple-step look-ahead method is presented. By following the laws, a US^3PR needing k-step to look ahead can be obtained. Compared with the results in [1]-[3], this work explores the multiple-step look-ahead DAP on more general net structures, namely α-nets and *binary* S^3PRs. Through analysis, it can be concluded that the conservative multiple-step look-ahead law in [1] is not applicable to an α-net. Therefore, the computing of a multiple-step look-ahead DAP on it needs to take more into consideration. It is shown that the number of look-ahead steps to check the safety of a state depends on the structure of a net model. Furthermore, a DAP on a class of S^3PR with two ξ-resources is presented. Through these expanded results, more objective rules about a multi-step look-ahead DAP on an S^3PR with ξ-resources begin to take shape.

The rest of the paper is organized as follows. Section II reviews some basic concepts and characterizations of Petri nets and S^3PR. Section III develops a multiple-step look-ahead DAP for a subclass of S^3PR namely an α-net. Meanwhile, the α-net is classified into two subclasses, which are α_1-net and α_2-net, respectively. By demonstrating examples, some rules and mathematical relations between the structures and their optimal DAP are presented. In Section IV, a DAP for an S^3PR with two ξ-resources is explored. We discuss some interesting problems regarding deadlock prevention and avoidance in Section V based on the findings of this research. Finally, some conclusions and future work are summarized in Section VI.

II. PRELIMINARIES

This section briefly presents pertinent definitions and notations for Petri nets [11], [37], S^3PR and ξ-resources.

A. BASIC DEFINITIONS OF PETRI NETS

A Petri net N is a four-tuple $N=(P, T, F, W)$, where P is a set of places and T is a set of transitions. P and T are finite, nonempty and disjoint sets, i.e., $P \neq \emptyset, T \neq \emptyset$, and $P \cap T = \emptyset$. $F \subseteq (P \times T) \cup (T \times P)$ is called the set of directed arcs from places to transitions or from transitions to places. W: $(P \times T) \cup (T \times P) \rightarrow \mathbb{N} = \{0, 1, 2, \cdots\}$ is a mapping that assigns a weight to each arc, i.e., if $f \in F$, $W(f)>0$; otherwise, $W(f) = 0$. W is called the weight function of a Petri net. From graph theory point of view, a Petri net is a bipartite digraph.

A marking M of a Petri net $N = (P, T, F, W)$ is a mapping: $P \rightarrow \mathbb{N}$. (N, M_0) is referred to as a net system or marked net with M_0 being the initial marking. For simplicity, a Petri net N with initial marking M_0 is denoted as (N, M_0) or (P, T, F, W, M_0). Let $p \in P$ be a place of a Petri net N. Place p is marked at M if $M(p) > 0$. A set of places $D \subseteq P$ is marked at M if at least one place in D is marked, viz., $\exists p \in D, M(p) > 0$. $M(D) = \sum_{p \in D} M(p)$ is the total number of tokens in D at M.

Let $x \in P \cup T$ be a node of a Petri net $N = (P, T, F, W)$. The preset of x, denoted by $^\bullet x$, is defined as $^\bullet x = \{y \in P \cup T \mid (y, x) \in F\}$ and its postset $x^\bullet$ is defined as $x^\bullet = \{y \in P \cup T \mid (x, y) \in F\}$. Given a place (transition) p (t), the elements in its preset are called the pre-transitions (pre-places) of p (t), while the postset of p (t) is named as post-transitions (post-places).

Let $N = (P, T, F, W)$ be a Petri net. A transition $t \in T$ is enabled at M if for all $p \in {^\bullet t}$, $M(p) \geqslant W(p, t)$, denoted by $M[t\rangle$. An enabled transition t can fire and and its firing transfers the Petri net to a new marking M' such that for all $p \in P$, $M'(p) = M(p) - W(p, t) + W(t, p)$, which is denoted as $M[t\rangle M'$. A Petri net is said to be free of self-loop if there do not exist a place p and a transition t such that $(p, t) \in F$ and $(t, p) \in F$. A self-loop-free Petri net can be represented by an incidence matrix $[N](p, t) = W(t, p) - W(p, t)$ that is an integer matrix indexed by P and T.

Marking M' is reachable from M_1 if there exist a feasible firing sequence of transitions (transition sequence for the sake of simplicity) $\sigma = t_1, t_2, \cdots, t_n$ and markings $M_2, \cdots, M_n$ such that $M_1[t_1\rangle M_2[t_2\rangle \cdots M_n[t_n\rangle M'$ holds. Given a Petri net (N, M_0), the set of markings generated from M_0 is called the reachability set of (N, M_0), denoted by $R(N, M_0)$.

A vector I: $P \longrightarrow \mathbb{Z}$ indexed by P with $\mathbb{Z}$ being the set of integers is called a P-vector. A P-vector I is called a P-invariant if $I^T[N] = 0^T$. It is called a P-semiflow if for all $p \in P, I(p) \geqslant 0$. Let I be a P-vector. $||I|| = \{p|I(p) > 0\}$ is called its support. A non-empty place subset $S \subseteq P$ is a siphon if ${}^\bullet S \subseteq S^\bullet$. A siphon S is minimal if the removal of any place from S makes the fallacy of ${}^\bullet S \subseteq S^\bullet$. A siphon is strict if it does not contain the support of a P-semiflow. The set of strict minimal siphons in a Petri net is denoted by Π.

A path α in a Petri net is a string of nodes, i.e., $\alpha = x_1x_2 \dots x_n$, where $x_i \in P \cap T$ and $i \in \{1, 2, \dots, n\}$. A circuit is a path with $x_1 = x_n$. A simple circuit is a circuit where no node can appear more than once except x_1 or x_n.

B. S^3PR Models

This section reviews the primary notions and properties of the system of simple sequential processes with resources, which is called S^3PR, defined from the standpoint of Petri nets [8]. It represents an important net type that can model a large class of automated manufacturing systems. Such a class of Petri nets has been extensively studied, due to its generality, perfect structural and behavioral properties.

Definition 1: A simple sequential process (S^2P) is a Petri net $N = (P_A \cup \{p^0\}, T, F)$, satisfying the following statements:

1) $P_A \neq \emptyset$ is called the set of activity (operation) places;
2) $p^0 \notin P_A$ is called the process idle place or idle place;
3) N is a strongly connected state machine;
4) Every circuit of N contains the place p^0.

Definition 2: An S^2P with resources (S^2PR) is a Petri net $N = (\{p^0\} \cup P_A \cup P_R, T, F)$, satisfying

1) The subnet generated from $X = P_A \cup \{p^0\} \cup T$ is an S^2P.
2) $P_R \neq \emptyset$, $(P_A \cup \{p^0\}) \cap P_R = \emptyset$.
3) $\forall p \in P_A, \forall t \in {}^\bullet p, \forall t' \in p^\bullet, \exists r_p \in P_R$, ${}^\bullet t \cap P_R = t'^\bullet \cap P_R = \{r_p\}$.
4) $\forall r \in P_R$, ${}^{\bullet\bullet} r \cap P_A = r^{\bullet\bullet} \cap P_A \neq \emptyset$; $\forall r \in P_R$, ${}^\bullet r \cap r^\bullet = \emptyset$.
5) ${}^{\bullet\bullet}(p^0) \cap P_R = (p^0)^{\bullet\bullet} \cap P_R = \emptyset$.

Definition 3: Given an S^2PR $N = (P_A \cup \{p^0\} \cup P_R, T, F)$, an initial marking M_0 is said to be acceptable for N if:

1) $M_0(p^0) \geq 1$;
2) $M_0(p) = 0, \forall p \in P_A$;
3) $M_0(r) \geq 1, \forall r \in P_R$.

Definition 4: An S^3PR, i.e., a system of S^2PR, can be defined recursively as follows:

1) An S^2PR is an S^3PR.
2) Let $N_i = (P_{A_i} \cup \{p_i^0\} \cup P_{R_i}, T_i, F_i)$ $(i \in \{1, 2\})$ be two S^3PR, satisfying $(P_{A_1} \cup \{p_1^0\}) \cap (P_{A_2} \cup \{p_2^0\}) = \emptyset$, $P_{R_1} \cap P_{R_2} = P_C \neq \emptyset$. A Petri net $N = (P_A \cup \{p^0\} \cup P_R, T, F)$ composed of N_1 and N_2 through P_C is still an S^3PR, defined as $P_A = P_{A_1} \cup P_{A_2}$, $P^0 = \{p_1^0\} \cup \{p_2^0\}$, $P_R = P_{R_1} \cup P_{R_2}$, $T = T_1 \cup T_2$, and $F = F_1 \cup F_2$.

Given a resource $r \in P_R$ in an S^3PR, the set of holders of r is denoted as $H(r) = ({}^{\bullet\bullet} r) \cap P_A$. For a siphon S in an S^3PR, $S = S^R \cap S^A$, where $S^R = S \cap P_R$ and $S^A = S \cap P_A$.

C. RT-CIRCUIT AND ξ-RESOURCE

Let θ be a directed circuit in an S^3PR. It is called a resource-transition circuit (RT-circuit) if it contains resource places and transitions only. Let $T(\theta)$ and $R(\theta)$ denote the sets of all transitions and resource places in θ, respectively. Let ${}^{\langle p \rangle}t$ and $t^{\langle p \rangle}$ denote the input and output operation place of t, respectively. Similarly, Let ${}^{\langle t \rangle}p$ and $p^{\langle t \rangle}$ denote the input and output transitions of p, respectively. By the structural properties of an S^3PR, each transition has a unique input operation place and a unique output operation place, i.e., both ${}^{\langle p \rangle}t$ and $t^{\langle p \rangle}$ are unique in an S^3PR. An RT-circuit is said to be *perfect* if it satisfies $({}^{\langle p \rangle}T(\theta))^\bullet = T(\theta)$, by defining ${}^{\langle p \rangle}T(\theta) = \bigcup_{t \in T(\theta)} \{{}^{\langle p \rangle}t\}$. A *perfect* RT-circuit (PRT-circuit) in an S^3PR (N, M_0) is said to be saturated at a marking $M \in R(N, M_0)$ if $M({}^{\langle p \rangle}T(\theta)) = \psi(R(\theta)) = \sum_{r \in R(\theta)} \psi(r)$, where $\psi(r)$ is the capacity of the resource r, i.e., $\psi(r) = M_0(r)$. When a maximal *perfect* RT-circuit (MPRT-circuit) is saturated, deadlocks occur in an S^3PR [2], [3].

In an S^3PR, a resource is called a ξ-resource if it is of one-unit (capacity) and is shared by two or more MPRT-circuits that do not contain each other. In fact, it is proved that, in an S^3PR without ξ-resource, there exist only two types of reachable markings: deadlock and non-deadlock (safe) markings [2]. The safe markings are states belonging to the live zone (LZ) [7] that, from the viewpoint of the reachability graph, forms the maximal strongly connected component including the initial marking.

Definition 5: Given an S^3PR (N, M_0), suppose that there exist two RT-circuits θ_1 and θ_2 such that $R(\theta_1) \cap R(\theta_2) = \{r\}$. Resource r is called a ξ-resource if $M_0(r) = 1$.

Definition 6: Given an S^3PR (N, M_0), $r \in P_R$ is said to be independent if there does not exist a strict minimal siphon S, such that $H(r) \cap S^A \neq \emptyset$; otherwise, r is said to be dependent. Let S_{in}^R denote the set of independent resources in P_R.

Definition 7: Given a resource $r \in P_R$ in an S^3PR, a holder-resource circuit (HR-circuit) associated with r, denoted by $\mathcal{H}(r)$, is a simple circuit containing r as the unique resource place, an activity place $p \in H(r)$ and transitions. An HR-circuit $\mathcal{H}(r)$ is said to be monoploid if $r \in S_{in}^R$.

To help clarify the above definitions [1], Fig. 1 illustrates an S^3PR, where there are nine RT-circuits, including $p_{12}t_{13}p_{13}t_2p_{12}$, $p_{13}t_{12}p_{15}t_{11}p_{16}t_4p_{14}t_3p_{13}$, $p_{16}t_{10}p_{17}t_7p_{16}$, $p_{16}t_{10}p_{17}t_5p_{16}$, $p_{12}t_{13}p_{13}t_{12}p_{15}t_{11}p_{16}t_4p_{14}t_3p_{13}t_2p_{12}$, $p_{13}t_{12}p_{15}t_{11}p_{16}t_{10}p_{17}t_7p_{16}t_4p_{14}t_3p_{13}$, $p_{13}t_{12}p_{15}t_{11}p_{16}t_{10}p_{17}t_5p_{16}t_4p_{14}t_3p_{13}$, $p_{12}t_{13}p_{13}t_{12}p_{15}t_{11}p_{16}t_{10}p_{17}t_7p_{16}t_4p_{14}t_3p_{13}t_2p_{12}$ and $p_{12}t_{13}p_{13}t_{12}p_{15}t_{11}p_{16}t_{10}p_{17}t_5p_{16}t_4p_{14}t_3p_{13}t_2p_{12}$.

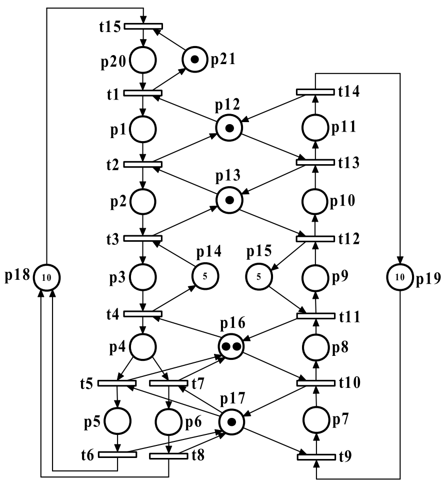

FIGURE 1. An S^3PR net.

According to Definition 5, p_{13} is the unique ξ-resource in this S^3PR. Note that p_{16} is not a ξ-resource since $M_0(p_{16}) > 1$. There are 6 strict minimal siphons in this model, one of which is $S = \{p_4, p_{10}, p_{13}, p_{14}, p_{15}, p_{16}\}$. According to Definition 6, p_{14}, p_{15} and p_{21} are independent resources, i.e., $S^R_{in} = \{p_{14}, p_{15}, p_{21}\}$. Moreover, there are 13 HR-circuits in this model, such as $p_{12}t_1p_1t_2p_{12}$ and $p_{17}t_5p_5t_6p_{17}$. However, only $p_{14}t_3p_3t_4p_{14}$, $p_{15}t_{11}p_9t_{12}p_{15}$ and $p_{21}t_{15}p_{20}t_1p_{21}$ are monoploid.

III. DAP FOR α-NET

It is shown in [1] that for a class of S^3PR, namely a unitary S^3PR (US^{3}PR) with one ξ-resource, the deadlock avoidance problem can be solved by a multi-step look-ahead DAP and it is of polynomial complexity. Definition 8 below describes the US^{3}PR in detail. Based on this model, the results obtained in [1] are extended in this paper. In this section, different from US^{3}PR, a kind of S^3PR with a ξ-resource, namely an α-net, is presented along with its DAP. Some relationships between the number of steps needed to look ahead, denoted by $\mathcal{K}$, and the resource configuration are revealed, verified and proved. Definition 9 and 10 classify the independent resources and monoploid HR-circuits. On the basis of that, the definition of an α-net is presented in Definition 11.

Definition 8: An S^3PR (N, M_0) is said to be unitary if there is only one ξ-resource and for all $r \in P_R$, there exists an RT-circuits θ, such that $r \in R(\theta)$, where P_R is a set of resource places in N.

Definition 9: Given an S^3PR (N, M_0) with n RT-circuits $\theta_1, \theta_2, \cdots, \theta_n$, let S^R_{in} be the set of independent resources in N, where $S^R_{in} \subseteq P_R$. Let $\mathcal{S}^R_{sin} = \{r | r \in S^R_{in} \cap (P_R \setminus \bigcup_{i=1}^{n} R(\theta_i))\}$. $\mathcal{S}^R_{sin} \subseteq S^R_{in}$ is said to be the set of strongly independent resources of N. $\mathcal{S}^R_{win} = S^R_{in} \setminus \mathcal{S}^R_{sin}$ is said to be the set of weakly independent resources of N.

Definition 10: A monoploid HR-circuit $\mathcal{H}(r)$ is denoted by $\mathcal{H}^s(r)$ if $r \in \mathcal{S}^R_{sin}$, namely a strongly monoploid HR-circuit. It is denoted by $\mathcal{H}^w(r)$ if $r \in \mathcal{S}^R_{win}$, namely a weakly monoploid HR-circuit.

Definition 11: Let $\mathcal{S}^R_{sin} \neq \emptyset$ be the set of strongly independent resources in an S^3PR (N, M_0) with $N = (P^0 \cup P_A \cup P_R, T, F, W)$. (N, M_0) is called an α-net if it has only one ξ-resource.

To help understanding Definitions 9 and 10, consider the marked S^3PR again in Fig. 1. It is not a US^{3}PR since resource place p_{21} does not belong to any of the nine RT-circuits. As for the independent resources, i.e., $S^R_{in} = \{p_{14}, p_{15}, p_{21}\}$, it can be concluded that only p_{21} is strongly independent in this model. In other words, $\mathcal{S}^R_{sin} = \{p_{21}\}$ and $\mathcal{S}^R_{win} = \{p_{14}, p_{15}\}$. According to Definition 11, this S^3PR is an α-net. The relationship among the resources in an α-net is depicted by the Venn diagram in Fig. 2.

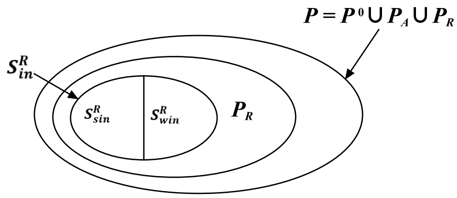

FIGURE 2. Inclusion relationship among strongly (weakly) independent resource sets in an α-net.

According to Definition 11, an α-net contains at least a strongly monoploid HR-circuit. As for weakly monoploid HR-circuits, since $\mathcal{S}^R_{win} = \emptyset$ is acceptable, an α-net does not necessarily contain a weakly independent resource. According to the definitions of US^{3}PRs [1] and α-nets, it can be concluded that: First, as sub-nets of S^3PRs, both of these two models contain only one ξ-resource and a number of HR-circuits. Second, since an α-net without any strongly monoploid HR-circuit can be regarded as a US^{3}PR, we consider that US^{3}PR is a subclass of α-nets.

By the structural features, α-nets can be divided into two subclasses, denoted as α_1-nets and α_2-nets. In the following subsections, we give their definitions and study their optimal DAP respectively.

A. DAP OF α_1-NET

Definition 12: Let $\mathcal{H}^s(r)$ be an arbitrary strongly monoploid HR-circuit in an α-net (N, M_0). (N, M_0) is said to be an α_1-net if for all $p \in \mathcal{H}^s(r)$, $|^{\langle t \rangle}(p^{\bullet\bullet} \cap P_A)| \leq 1$, where $^{\langle t \rangle}(p^{\bullet\bullet} \cap P_A) = \bigcup_{x \in p^{\bullet\bullet} \cap P_A}^{\langle t \rangle} x$ and P_A is the set of operation places in N.

Note that $|^{\langle t \rangle}(p^{\bullet\bullet} \cap P_A)| = 0$ is feasible, which implies that $^{\langle t \rangle}(p^{\bullet\bullet} \cap P_A) = \emptyset$. That is to say, in an α_1-net, there may exist a place $p \in \mathcal{H}^s(r)$ such that $p^{\bullet\bullet} \cap P_A = \emptyset$ holds. In other cases, $|^{\langle t \rangle}(p^{\bullet\bullet} \cap P_A)| = 1$, implying $p^{\bullet\bullet} \cap P_A \neq \emptyset$.

Next, some examples and their simulation results are presented to illustrate these characteristics. Fig. 3 shows a parameterized α_1-net which contains a strongly monoploid HR-circuit $\mathcal{H}^s(r)$, i.e., $\mathcal{H}^s(r) = t_1p_1t_2p_9t_1$. In Fig. 3,

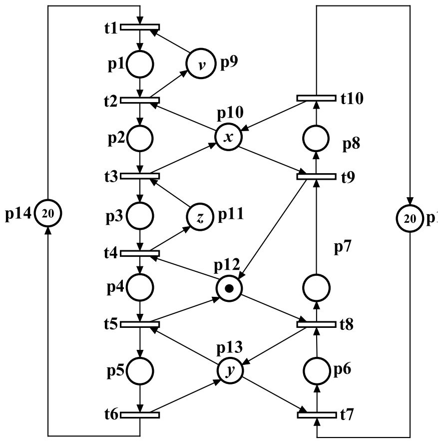

FIGURE 3. A parameterized α_1-net.

the initial marking is given as follows. For the independent resource places, $M_0(p_9) = v$ and $M_0(p_{11}) = z$ ($v, z \in \mathbb{N}^+$). For other resource places, we set $M_0(p_{10}) = x$ and $M_0(p_{13}) = y$ ($x, y \in \mathbb{N}^+$). In particular, to make this model include a ξ-resource initially, we have $M_0(p_{12}) = 1$.

Each idle places has 20 tokens, while the holder places carry no resource. In [1], it is shown that, in an S^{3}PR, the idle places with enough tokens at the initial marking do not affect the number of steps to look ahead for checking the safety of a marking. Thus, for convenience, we remove the idle places and the corresponding arcs associated with them and consider the reduced version only as shown in Fig. 4.

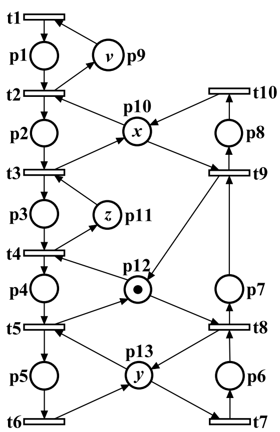

FIGURE 4. A reduced parameterized α_1-net.

In Fig. 4, we aim to find the relation between $\mathcal{K}$ and the four parameters v, z, x and y for an optimal DAP, i.e., for checking the safety of a reachable marking. The result is presented in Table 1. Note that hereafter we use "$\times$" to denote an arbitrary integer that can be applied to a parameter which has no effect on $\mathcal{K}$. Apparently, none of the three parameters, i.e., $M_0(p_{11})$, $M_0(p_{10})$ and $M_0(p_{13})$, can impact $\mathcal{K}$. Thus z, x and y here can be an arbitrary positive integer. In fact, $\mathcal{K} = v + 2$ is always true in this case. Moreover, we should point out that the simulations on $M_0(p_{10})$ and $M_0(p_{13})$ are

TABLE 1. Simulation results of Fig. 4.

$M_0(p_9) = v$	1	2	3	5	10	20	50	70	90
$M_0(p_{11}) = z$	×	×	×	×	×	×	×	×	×
$M_0(p_{10}) = x$	×	×	×	×	×	×	×	×	×
$M_0(p_{13}) = y$	×	×	×	×	×	×	×	×	×
$\mathcal{K}$	3	4	5	7	12	22	52	72	92

in accord with the result in [1]. That is to say, in a US^{3}PR, the dependent non-ξ-resources do not affect $\mathcal{K}$ as well. Meaningfully, if the unique strongly monoploid HR-circuit $\mathcal{H}^s(r)$ in Fig. 4 is removed from this model, according to [1], $\mathcal{K} = 2$ holds. Therefore, it is natural to suppose that there exists a linear relation between the parameter $\mathcal{K}$ of this model and the initial marking of the resource in the strongly monoploid HR-circuit $\mathcal{H}^s(r)$. In order to further confirm this finding, in what follows, we test it by using some other typical α_1-nets, which will help us derive the expected relationship between $\mathcal{K}$ and the initial resource configuration.

A more complex example is shown in Fig. 5 (a) with an initial token distribution. There are six parameters, i.e., $M_0(p_{11}) = v, M_0(p_{12}) = u, M_0(p_{14}) = z_1, M_0(p_{15}) = z_2, M_0(p_{13}) = x$ and $M_0(p_{17}) = y$. In this model, we focus on the relationship between $\mathcal{K}$ and these parameters. The test results are shown in Table 2. Similar to Fig. 4, it is clear that we can leave $M_0(p_{14}), M_0(p_{15}), M_0(p_{13})$ and $M_0(p_{17})$ out of consideration. The relationship between the number

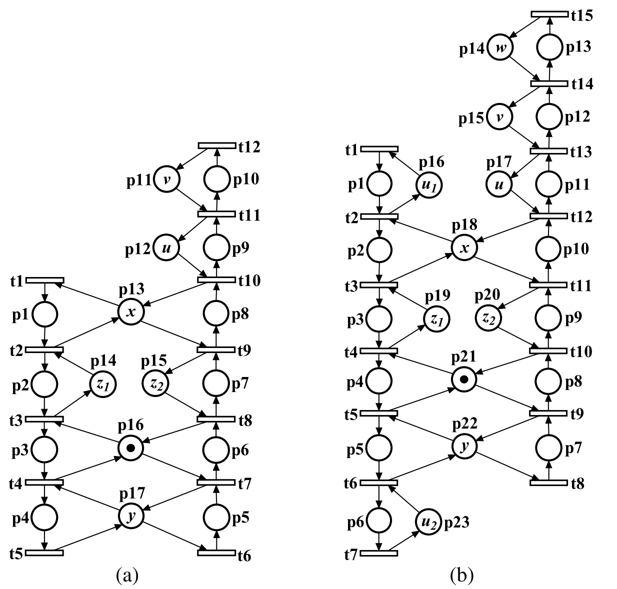

FIGURE 5. Two reduced parameterized α_1-nets.

TABLE 2. Simulation results of Fig. 5 (a).

$M_0(p_{11}) = v$	1	1	2	5	10	20	30	50	80
$M_0(p_{12}) = u$	1	2	1	10	5	30	20	80	50
$M_0(p_{14}) = z_1$	×	×	×	×	×	×	×	×	×
$M_0(p_{15}) = z_2$	×	×	×	×	×	×	×	×	×
$M_0(p_{13}) = x$	×	×	×	×	×	×	×	×	×
$M_0(p_{17}) = y$	×	×	×	×	×	×	×	×	×
$\mathcal{K}$	6	8	7	28	23	83	73	213	183

of look-ahead steps and the parameters $M_0(p_{11})$ and $M_0(p_{12})$ can be derived, though it is not intuitive. According to Table 2, the analytical expression of v, u and $\mathcal{K}$ satisfies $\mathcal{K} = v + 2u + 3$, where the constant 3 may stem from the sub-net without the two strongly monoploid HR-circuits, i.e., $t_{12}p_{11}t_{11}p_{10}t_{12}$ and $t_{11}p_{12}t_{10}p_9t_{11}$ in Fig. 5 (a). To show the relationship between the number of look-ahead steps and the parameters in this kind of model more clearly, a study on the third example is conducted.

The model in Fig. 5 (b) is obtained by extending the one in Fig. 5 (a). In Fig. 5 (b), there are five strongly monoploid HR-circuits. We have nine parameters in this α_1-net, i.e., $M_0(p_{14}) = w, M_0(p_{15}) = v, M_0(p_{17}) = u$, $M_0(p_{16}) = u_1, M_0(p_{19}) = z_1, M_0(p_{20}) = z_2, M_0(p_{23}) = u_2$, $M_0(p_{18}) = x$ and $M_0(p_{22}) = y$. According to the above examples, $\mathcal{K}$ is likely to be affected by u, u_1, u_2, v and w. To figure it out, according to the experimental results given in Table 3, $\mathcal{K} = w + 2v + 3u + u_1 + u_2 + 3$. It seems that once there are two or more strongly monoploid HR-circuits, there exists a first-order polynomial relation between $\mathcal{K}$ and the related parameters. Furthermore, for each unknown in the polynomial, i.e., the initial marking of $r \in \mathcal{S}^R_{sin}$, the coefficients of the unknowns depend on the location of the strongly monoploid HR-circuit.

TABLE 3. Simulation results of Fig. 5 (b).

$M_0(p_{14}) = w$	1	2	1	2	1	3	10	1	1
$M_0(p_{15}) = v$	2	1	2	2	2	1	12	1	1
$M_0(p_{16}) = u_1$	1	1	1	1	2	1	3	5	10
$M_0(p_{17}) = u$	1	1	2	1	2	1	5	10	5
$M_0(p_{19}) = z_1$	×	×	×	×	×	×	×	×	×
$M_0(p_{20}) = z_2$	×	×	×	×	×	×	×	×	×
$M_0(p_{23}) = u_2$	1	1	1	1	2	3	1	1	5
$M_0(p_{18}) = x$	×	×	×	×	×	×	×	×	×
$M_0(p_{22}) = y$	×	×	×	×	×	×	×	×	×
$\mathcal{K}$	13	12	16	14	18	15	56	42	36

Based on the above analysis, two results are summarized as follows. According to a reduced parameterized α_1-net shown in Fig. 7, first, this class of α-net can be divided into two parts: one containing the strongly monoploid HR-circuits and the other is $\mathcal{H}^s(r)$-free, called the H-component and R-component, respectively. Note that the R-component is a sub-net of an α_1-net, where there is no strongly monoploid HR-circuit. Each of these two parts contributes partially to $\mathcal{K}$, denoted by $\mathcal{K}_H$ and $\mathcal{K}_R$, respectively. Accordingly, we have $\mathcal{K} = \mathcal{K}_R + \mathcal{K}_H$. The R-component is clearly a US^{3}PR, according to Definition 8. Since the resource configuration of the monoploid HR-circuits within the R-component does not affect $\mathcal{K}_R$, the parameters of the initial marking in the corresponding resource places, i.e., z_{ij} ($i \in \{1, 2, 3, 4\}, j \in \{1, 2, \cdots\}$), can be arbitrary positive integers. m, n, p and q represent the numbers of weakly monoploid HR-circuits in the R-component ($m, n, p, q \in \mathbb{N}$). x and y denote the initial markings of the two dependent non-ξ-resources and can be arbitrary positive integers as well. As shown in Fig. 7, such a partition in a US^{3}PR is reasonable due to the uniqueness of the ξ-resource.

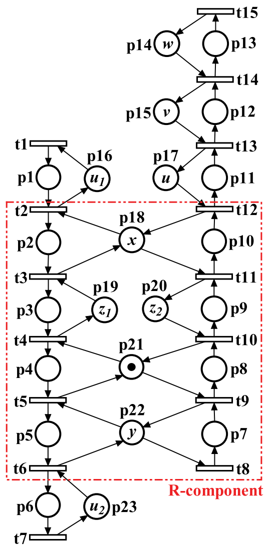

FIGURE 6. R-component of the α_1-net in Fig. 5 (b).

On the basis of the above discussion, $\mathcal{K}_R = max\{n+2, p+2\}$, where n and p represent the numbers of the weakly monoploid HR-circuits that are structurally associated with the ξ-resource, as shown in Fig. 7. For details, one can refer to the work in [1]. However, to help clarify this statement, we give an example. As shown in Fig. 6, the R-component (sub-net of this α_1-net but without any strongly monoploid HR-circuit) of the model in Fig. 5 (b) is boxed in red. According to [1], n and p are the numbers of weakly monoploid HR-circuits within the R-component of this net. Since $p_{20}t_{11}p_9t_{10}p_{20}$ is the only weakly monoploid HR-circuit on the right side of the RT-circuit $p_{18}t_{11}p_{20}t_{10}p_{21}t_4p_{19}t_3p_{18}$, we have $n = 1$. However, in the RT-circuit $p_{21}t_9p_{22}t_5p_{21}$, there is no weakly independent resource. Therefore, $p = 0$. Thus, $\mathcal{K}_R = max\{n+2, p+2\} = 3$ holds.

Second, for the H-component, it consists of four sub-parts, namely H_1, H_2, H_3 and H_4. Each of the four sub-parts generates $\mathcal{K}_{H_1}, \mathcal{K}_{H_2}, \mathcal{K}_{H_3}$ and $\mathcal{K}_{H_4}$ steps that need to look ahead, and therefore, $\mathcal{K}_H = \mathcal{K}_{H_1} + \mathcal{K}_{H_2} + \mathcal{K}_{H_3} + \mathcal{K}_{H_4}$. Moreover, these four parts contain $\omega_1, \omega_2, \omega_3$ and ω_4 strongly monoploid HR-circuits, respectively. As for the resource allocation among these strongly monoploid HR-circuits, there are ψ_{ij} ($i \in \{1, 2, 3, 4\}, j \in \{1, 2, \cdots, \omega_i\}$) tokens distributing in the strongly independent resources, as shown in Fig. 7. Based on that, the following four equations hold.

$$\begin{aligned}
\mathcal{K}_{H_1} &= \psi_{11} + 2\psi_{12} + \cdots + \omega_1\psi_{1\omega_1} = \sum_{i=1}^{\omega_1} i\psi_{1i} \\
\mathcal{K}_{H_2} &= \psi_{21} + 2\psi_{22} + \cdots + \omega_2\psi_{2\omega_2} = \sum_{i=1}^{\omega_2} i\psi_{2i} \\
\mathcal{K}_{H_3} &= \psi_{31} + 2\psi_{32} + \cdots + \omega_3\psi_{3\omega_3} = \sum_{i=1}^{\omega_3} i\psi_{3i} \\
\mathcal{K}_{H_4} &= \psi_{41} + 2\psi_{42} + \cdots + \omega_4\psi_{4\omega_4} = \sum_{i=1}^{\omega_4} i\psi_{4i} \qquad (1)
\end{aligned}$$

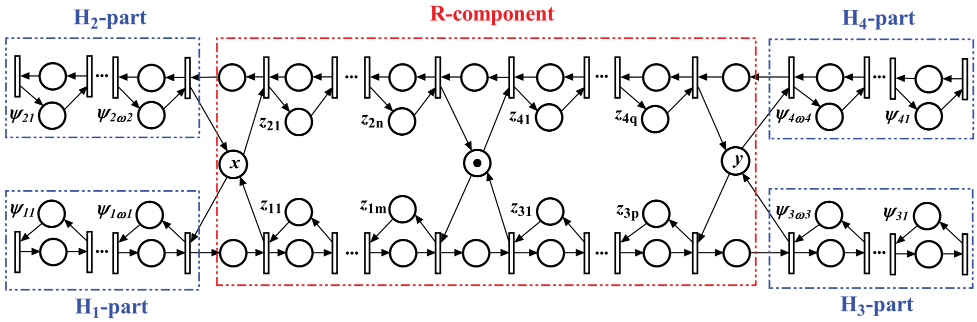

FIGURE 7. A general reduced parameterized α_1-net.

On the basis of the above analysis, we have the following result.

Proposition 1: Given an α_1-net (N, M_0), an optimal DAP $\mathcal{K}$ satisfies

$$\mathcal{K} = \mathcal{K}_R + \mathcal{K}_H = max\{n+2, p+2\} + \sum_{j=1}^{4}(\sum_{i=1}^{\omega_j} i\psi_{ji}) \quad (2)$$

where

- n and p are the numbers of weakly monoploid HR-circuits within the R-component in N ($n, p \in \mathbb{N}$);
- ω_j ($j \in \{1, 2, 3, 4\}$) is the number of strongly monoploid HR-circuits in H_j ($j \in \{1, 2, 3, 4\}$) within the H-component in N ($\omega_j \in \mathbb{N}$);
- ψ_{ji} ($i \in \{1, 2, \cdots, \omega_j\}, j \in \{1, 2, 3, 4\}$) is the initial marking of a corresponding strongly monoploid resource place within the H-component in N ($\psi_{ji} \in \mathbb{N}^+$).

Proof: First, for the R-component, considering the initial markings of the two non-ξ-resources in N, parameters x and y have no effect on $\mathcal{K}_R$. The conclusion of this statement is presented in [1]. Thus, $\mathcal{K}_R = max\{n+2, p+2\}$ holds.

Next, for the H-component, it can be proved through the structural analysis and the transmission of tokens. Suppose that there is a set of correlative HR-circuits in this part of the S^3PR. As mentioned in [2], the deadlock problem is characterized by a *perfect* resource-transition circuit that is saturated at a reachable marking, which implies that, for all post-operation places of the transitions in an RT-circuit, if their token sum is equal to the capacity of the resource places within this circuit, it is said to be saturated. That is, at the states in DZ* [1], i.e., a sub-set of states that belong to the dead zone (DZ) [7], no strict minimal siphon of the Petri net is emptied, and for each RT-circuit, at least one resource place is not emptied. Particularly, this resource is exactly the ξ-resource in the α_1-net. However, for the states other than DZ* in DZ, on the contrary, there exists an emptied resource place in an RT-circuit of an α_1-net. Moreover, for the dead markings, two *perfect* RT-circuits are both emptied.

We first consider the part H_1. In H_1, $\psi_{11}, \psi_{12}, \cdots, \psi_{1\omega_1}$ (suppose $\psi_{1i} > 1$ and $i \in \{1, 2, \cdots, \omega_1\}$) are the initial markings of the corresponding strongly monoploid resource places. For the resource place that contains ψ_{11} tokens as its initial marking, denoted as r_1, with the help of its post-transitions, it needs ψ_{11} times of transition firings to make it emptied. Meanwhile, the resource place that contains ψ_{12} tokens, denoted as r_2, needs ψ_{12} times to make its corresponding holder place hold ψ_{12} tokens. However, different from r_1, for r_2, there are also ψ_{12} tokens that flow to r_1 simultaneously. Hence, it needs another ψ_{12} times to empty r_1, in the procedure of emptying r_2. Overall, in this case, r_2 needs $2\psi_{12}$ times to be emptied thoroughly. By analogy, from resource places that contain $\psi_{11}, \psi_{12}, \cdots, \psi_{1\omega_1}$ tokens, there need $\psi_{11}, 2\psi_{12}, 3\psi_{13}, \cdots, \omega_1\psi_{1\omega_1}$ times of transition firings to empty the resource places, respectively. Clearly, there is a relationship between $\mathcal{K}$ and all parameters in H_1 part. That is to say, $\mathcal{K}_{H_1}$ is the linear combination of $\psi_{11}, \psi_{12}, \cdots, \psi_{1\omega_1}$. Thus, $\mathcal{K}_{H_1} = \psi_{11} + 2\psi_{12} + \cdots + \omega_1\psi_{1\omega_1} = \sum_{i=1}^{\omega_1} i\psi_{1i}$ holds.

Iteratively, this principle holds in H_2, H_3 and H_4 as well. Thus, we have $\mathcal{K}_H = \mathcal{K}_{H_1} + \mathcal{K}_{H_2} + \mathcal{K}_{H_3} + \mathcal{K}_{H_4} = \sum_{i=1}^{\omega_1} i\psi_{1i} + \sum_{i=1}^{\omega_2} i\psi_{2i} + \sum_{i=1}^{\omega_3} i\psi_{3i} + \sum_{i=1}^{\omega_4} i\psi_{4i} = \sum_{j=1}^{4}(\sum_{i=1}^{\omega_j} i\psi_{ji})$ and accordingly $\mathcal{K} = \mathcal{K}_R + \mathcal{K}_H = max\{n+2, p+2\} + \sum_{j=1}^{4}(\sum_{i=1}^{\omega_j} i\psi_{ji})$. □

In summary, this subsection discusses a formal constructive method of a DAP for a kind of α-net, namely α_1-net. First, it shows that the *conservation law* [1] partially holds in this kind of model. In plain words, the R-component of the α_1-net keeps its speciality with US^3PR, i.e., the initial marking of a weakly independent resource does not affect $\mathcal{K}$ for an optimal DAP. Second, for the H-component, four equations illustrate the relation among the structure, resource configuration and $\mathcal{K}$. As for this relationship, there is a summative equation to indicate that the total $\mathcal{K}$ is dependent on both the H-component and the R-component. That is to say, the structure of an α_1-net is the key to figure out its optimal DAP by looking ahead. Once the structure and the initial resource configuration are fixed, the number of look-ahead steps for an optimal DAP is determined as well.

B. DAP FOR α_2-NET

This subsection introduces another kind of α-net that has multiple branches in a process and analyzes the number of steps to look-ahead for its optimal DAP, namely α_2-net. According to the definitions and characteristic in Definition 13, as a subclass of α-net, there is a difference between an α_2-net and an α_1-net.

Definition 13: An α-net (N, M_0) is said to be an α_2-net if there exists a place $p \in \mathcal{H}^s(r)$ such that $|^{\langle t \rangle}(p^{\bullet\bullet} \cap P_A)| > 1$, where $^{\langle t \rangle}(p^{\bullet\bullet} \cap P_A) = \bigcup^{\langle t \rangle}_{x \in p^{\bullet\bullet} \cap P_A} x$ and P_A is the set of operation places in N.

The difference between Definitions 13 and 12 (α_1-net) is mainly the cardinality of the transition set, i.e., $^{\langle t \rangle}(p^{\bullet\bullet} \cap P_A)$. In fact, in an α_2-net, there exists a place p that belongs to a strongly monoploid HR-circuit, such that $|^{\langle t \rangle}(p^{\bullet\bullet} \cap P_A)| = \lambda$, where $\lambda = \{2, 3, \cdots\}$. On the basis of the value of λ, α_2-nets can be classified and denoted as α_2^2-net, α_2^3-net, $\cdots$, α_2^λ-net, respectively, where $\lambda > 1$ and $\lambda \in \mathbb{N}$. For an α_2-net, λ can be regarded as the structural parameter, which represents the number of branches in its S^2P. Note that if $\lambda \leq 1$ in an α_2-net, it is actually an α_1-net by Definition 12.

As mentioned in the last section, the idle places can be removed from our study, since the final outcome depends on the resources only. For simplicity, hereinafter, we use α_2-net (α_2^λ-net) to denote the reduced one.

A simple parameterized and reduced α_2^2-net is used to illustrate the number of steps to look-ahead for a DAP in this kind of model. As shown in Fig. 8, according to Definition 13, $\lambda = 2$. Let $M_0(p_{14}) = 1$. Then, p_{14} is a ξ-resource. The token distribution for other resources is demonstrated above. Parameters $M_0(p_{10}), M_0(p_{12}), M_0(p_{13}), M_0(p_{11})$ and $M_0(p_{15})$ are denoted by v, z_1, z_2, x and y, respectively.

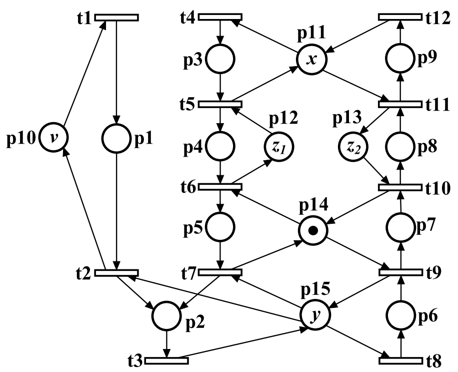

FIGURE 8. A parameterized α_2^2-net.

From the simulation results shown in Table 4, some properties can be revealed. Different from a US^{3}PR model, the initial marking of the strongly independent resource, i.e., $M_0(p_{10})$, has influence on $\mathcal{K}$ for a DAP. In this example, two rules can be summarized. The first is that $M_0(p_{12}), M_0(p_{13}), M_0(p_{11})$ and $M_0(p_{15})$ do not affect $\mathcal{K}$. Second, the relationship between $\mathcal{K}$ and v is $\mathcal{K} = v + 3$. It seems that there exists some mathematical relation between the number of steps to look-ahead and the structure of this model.

TABLE 4. Simulation results of Fig. 8.

$M_0(p_{10}) = v$	1	2	10	50	100	120	150	200
$M_0(p_{12}) = z_1$	×	×	×	×	×	×	×	×
$M_0(p_{13}) = z_2$	×	×	×	×	×	×	×	×
$M_0(p_{11}) = x$	×	×	×	×	×	×	×	×
$M_0(p_{15}) = y$	×	×	×	×	×	×	×	×
$\mathcal{K}$	4	5	13	53	103	123	153	203

Next, more examples are used to expound the rules behind the models. As shown in Fig. 9, the model is extended from Fig. 8 by adding a strongly monoploid HR-circuit in the process. Parameters $M_0(p_{11}), M_0(p_{13}), M_0(p_{14}), M_0(p_{15}), M_0(p_{12})$ and $M_0(p_{17})$ are denoted by v, z_1, z_2, u, x and y, respectively. Table 5 presents the simulation results.

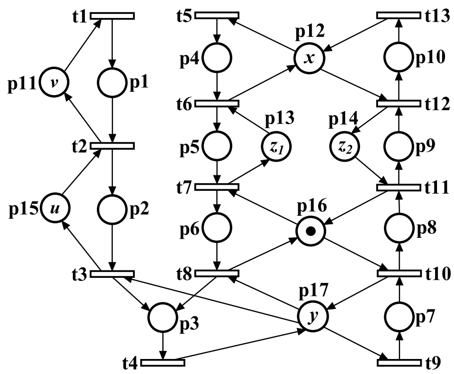

FIGURE 9. A parameterized α_2^2-net.

TABLE 5. Simulation results of Fig. 9.

$M_0(p_{11}) = v$	1	2	1	2	5	10	20	50	100
$M_0(p_{15}) = u$	1	1	2	2	6	12	18	60	120
$M_0(p_{13}) = z_1$	×	×	×	×	×	×	×	×	×
$M_0(p_{14}) = z_2$	×	×	×	×	×	×	×	×	×
$M_0(p_{12}) = x$	×	×	×	×	×	×	×	×	×
$M_0(p_{17}) = y$	×	×	×	×	×	×	×	×	×
$\mathcal{K}$	6	7	8	9	20	37	59	173	343

By comparing Tables 5 with 4, the relation between the number of steps to look-ahead and these parameters is $\mathcal{K} = v + 2u + 3$. Clearly, it is easy to figure out that $M_0(p_{13}), M_0(p_{14}), M_0(p_{12})$ and $M_0(p_{17})$ have no effect on $\mathcal{K}$ for an optimal DAP either. Let us further consider the model in Fig. 10. As usual, $M_0(p_{12})$, $M_0(p_{14})$, $M_0(p_{15})$, $M_0(p_{16})$, $M_0(p_{17})$, $M_0(p_{13})$ and $M_0(p_{19})$ are parameterized as w, v, z_1, z_2, u, x and y, respectively.

The relationship between $\mathcal{K}$ and these parameters are given in Table 6. Apparently, by observing this table, it can be found that a relationship exists between $\mathcal{K}$ and w, v and u, which is $\mathcal{K} = w + 2v + 3u + 3$. By inference, when the number of strongly monoploid HR-circuits increases, it can still be confirmed that $\mathcal{K}$ can be calculated by using a linear function of the partial parameters. Consequently, a more general illustration is depicted Fig. 11.

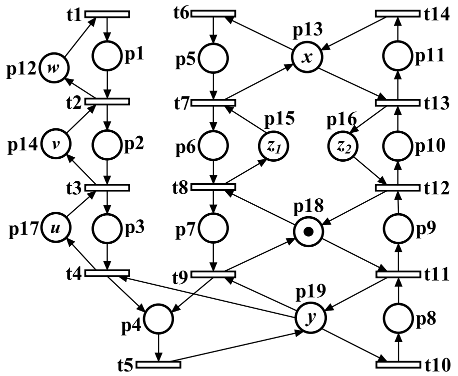

FIGURE 10. A parameterized α_2^2-net.

TABLE 6. Simulation results of Fig. 10.

$M_0(p_{12}) = w$	1	1	1	2	3	3	3	4	6
$M_0(p_{14}) = v$	1	1	1	2	2	3	4	3	6
$M_0(p_{17}) = u$	1	2	3	2	3	3	3	4	6
$M_0(p_{15}) = z_1$	×	×	×	×	×	×	×	×	×
$M_0(p_{16}) = z_2$	×	×	×	×	×	×	×	×	×
$M_0(p_{13}) = x$	×	×	×	×	×	×	×	×	×
$M_0(p_{19}) = y$	×	×	×	×	×	×	×	×	×
$\mathcal{K}$	9	12	15	15	19	21	23	25	39

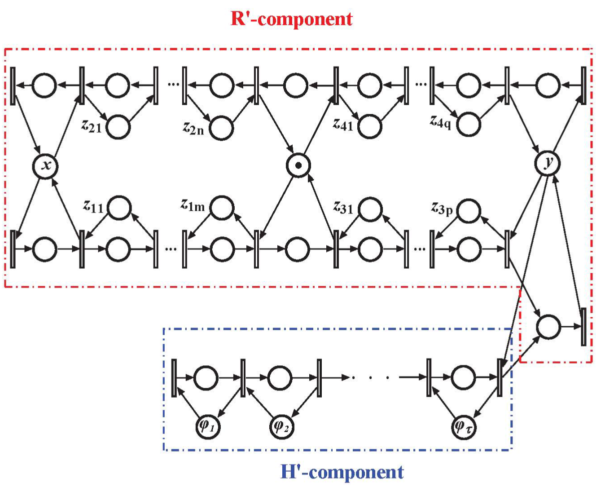

FIGURE 11. A parameterized α_2^2-net.

As shown in Fig. 11, a parameterized α_2^2-net is depicted. In this model, the α_2^2-net is divided into two parts that are denoted as the R′-component and H′-component, respectively. In the R′-component, m, n, p and q represent the numbers of weakly monoploid HR-circuits in the corresponding location. τ is the number of strongly monoploid HR-circuits, i.e., $\mathcal{H}^s(r)$ in the H′-component. $\varphi_1, \varphi_2, \cdots, \varphi_\tau$ represent the initial markings of these strongly monoploid HR-circuits, respectively. For the parameter z_{ij} $(i \in \{1, 2, 3, 4\}, j \in \{1, 2, \cdots\})$, due to the same reason elaborated in Fig. 7, as the initial marking in its corresponding resource, it represents the arbitrary positive integer. Parameters x and y are the initial markings of the two dependent non-ξ-resources and can be considered as arbitrary positive integers as well. Accordingly, we have the following result.

Proposition 2: Given an α_2^2-net (N, M_0), an optimal DAP $\mathcal{K}$ satisfies

$$\mathcal{K} = \sum_{i=1}^{\tau} i\varphi_i + max\{n+2, p+2\} \quad (3)$$

where

- n and p are the numbers of weakly monoploid HR-circuits within the R′-component in N $(n, p \in \mathbb{N})$;
- τ is the number of strongly monoploid HR-circuits within the H′-component in N $(\tau \in \mathbb{N})$;
- φ_i $(i \in \{1, 2, \cdots, \tau\})$ is the initial marking of the corresponding strongly monoploid resource place within the H′-component in N $(\varphi_i \in \mathbb{N}^+)$.

Proof: $\mathcal{K}$ can be divided into two parts. The first part is $\mathcal{K}_{R'}$ due to an $\mathcal{H}^s(r)$-free sub-net, i.e., the R′-component. The second part is $\mathcal{K}_{H'}$ induced by the H′-component. As previously mentioned, parameters x and y do not affect $\mathcal{K}_{R'}$. Therefore, $\mathcal{K}_{R'} = max\{n+2, p+2\}$ [1]. As for the H′-component, by analyzing the structure and token flow, the proof is similar to that given in Proposition 1. More specifically, the strongly monoploid resource place that contains φ_1 tokens, denoted as r_1', needs φ_1 times of transition firings to convey all resource units to its related holder place and then to be emptied. For the one that holds φ_2 resource units, denoted as r_2', in addition to φ_2 times of transition firings to its holder place, it also conveys φ_2 tokens to r_1' simultaneously, which requires extra φ_2 times of transition firings to empty r_1'. Thus, it takes $2\varphi_2$ times to empty r_2' completely.

By parity of reasoning, for the resource places that initially contain φ_3 or φ_4 token(s), it needs $3\varphi_3$ or $4\varphi_4$ times to be emptied. Iteratively, for the parameter φ_τ, the coefficient is $\tau\varphi_\tau$. Therefore, $\mathcal{K}_{H'} = \varphi_1 + 2\varphi_2 + 3\varphi_3 + 4\varphi_4 + \cdots + \tau\varphi_\tau$. In summary, $\mathcal{K} = \mathcal{K}_{R'} + \mathcal{K}_{H'} = \sum_{i=1}^{\tau} i\varphi_i + max\{n+2, p+2\}$.

□

Furthermore, in an α_2-net, we can still find solutions to calculate $\mathcal{K}$ in case of $\lambda > 2$. In order to solve this problem, a parameterized α_2^4-net is presented in Fig. 12, where $M_0(p_{14}) = w_1$, $M_0(p_{15}) = w_2$, $M_0(p_{16}) = v$, $M_0(p_{17}) = u_1$, $M_0(p_{18}) = u_2$, $M_0(p_{19}) = u_3$, $M_0(p_{21}) = z$, $M_0(p_{20}) = x$ and $M_0(p_{23}) = y$ are the parameters. To help figure $\mathcal{K}$ out in this α_2-net, Table 7 displays the final results.

By analyzing this example, it is obvious that only the resource places in the strongly monoploid HR-circuits have effect on $\mathcal{K}$. More specifically, $\mathcal{K} = w_1 + 2w_2 + v + u_1 + 2u_2 + 3u_3 + 2$ holds. This fully testifies the linear relationship between parameters in the H′-component and R′-component. Moreover, this kind of characteristics can be quantified to a first-order polynomial relation, i.e., in the H′-component, each strongly independent resource can affect $\mathcal{K}$ independently. Meanwhile in the R′-component, $\mathcal{K}_{R'}$ depends on its structure only. Particularly, for the latter, the initial marking of a weakly independent resource place does not affect $\mathcal{K}_{R'}$.

TABLE 7. Simulation results of Fig. 12.

$M_0(p_{14}) = w_1$	1	1	1	1	1	2	3	5	10
$M_0(p_{15}) = w_2$	1	3	1	1	1	2	5	5	10
$M_0(p_{16}) = v$	1	3	3	1	1	2	3	5	10
$M_0(p_{17}) = u_1$	1	1	1	1	2	2	3	5	10
$M_0(p_{18}) = u_2$	1	1	3	2	3	2	5	5	10
$M_0(p_{19}) = u_3$	1	1	1	3	4	2	3	5	10
$M_0(p_{21}) = z$	×	×	×	×	×	×	×	×	×
$M_0(p_{20}) = x$	×	×	×	×	×	×	×	×	×
$M_0(p_{23}) = y$	×	×	×	×	×	×	×	×	×
$\mathcal{K}$	12	20	18	20	26	22	40	52	102

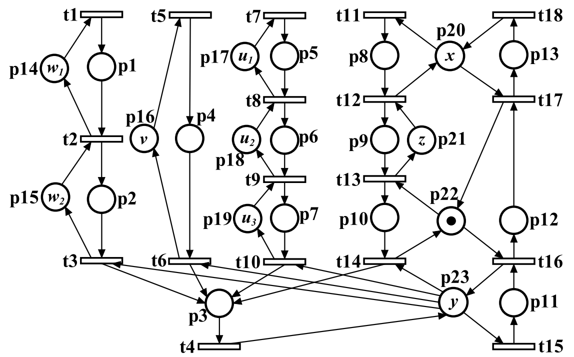

FIGURE 12. A parameterized α_2^4-net.

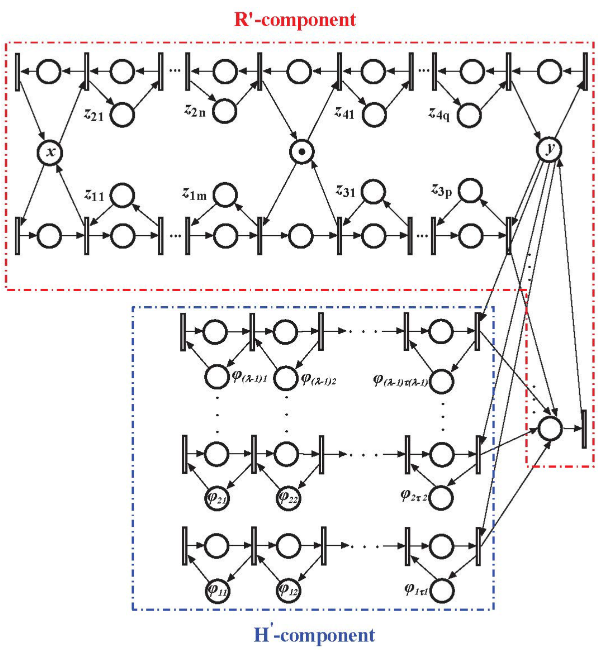

FIGURE 13. An α_2^λ-net.

Compared with the α_2^4-net in Fig. 12, Fig. 13 depicts an α_2^λ-net. Similar to Fig. 11, it is divided into the R′-component and H′-component as well. Specifically, in this parameterized α_2^λ-net, $\varphi_{i1}, \cdots, \varphi_{i\tau_i}(i = 1, 2, \cdots, \lambda - 1)$ represent the initial markings of the strongly independent resources in the H′-component. In the R′-component, as the initial marking of each weakly independent resource, the parameter z_{ij} $(i \in \{1, 2, 3, 4\}, j \in \{1, 2, \cdots\})$ can be regarded as the arbitrary positive integer. m, n, p and q represent the numbers of weakly monoploid HR-circuits. As in Propositions 1 and 2, the initial markings of dependent resources x and y are arbitrary positive integers. Based on this setting, we have the following result.

Proposition 3: Given an α_2^λ-net (N, M_0), an optimal DAP $\mathcal{K}$ satisfies

$$\mathcal{K} = \sum_{j=1}^{\lambda-1}\left(\sum_{i=1}^{\tau_j} i\varphi_{ji}\right) + max\{n+2, p+2\} \tag{4}$$

where

- n and p are the numbers of weakly monoploid HR-circuits within the R′-component in N $(n, p \in \mathbb{N})$;
- τ_j $(j \in \{1, 2, \cdots, (\lambda - 1)\})$ is the number of strongly monoploid HR-circuits of an S^2P within the H′-component in N $(\tau_j \in \mathbb{N})$;
- φ_{ji} $(i \in \{1, 2, \cdots, \tau_j\}, j \in \{1, 2, \cdots, (\lambda - 1)\})$ is the initial marking of a corresponding strongly monoploid resource place within the H′-component in N $(\varphi_{ji} \in \mathbb{N}^+)$.

Proof: The approach to prove this result is similar to the proof of the α_2^2-net given in Proposition 2. $\mathcal{K}$ is the sum of $\mathcal{K}_{R'}$ contributed by the R′-component and $\mathcal{K}_{H'}$ by the H′-component. $\mathcal{K}_{R'} = max\{n+2, p+2\}$ and its proof can be referred to Proposition 2. For simplicity, we consider the H′-component only. Through the analysis, each branch of the S^2P, which contains sets of strongly independent resources, is independent of each other in the H′-component on contributing $\mathcal{K}$. Thus, the total $\mathcal{K}_{H'}$ is the sum of steps that are generated from each branch of the S^2P in the H′-component, i.e., $\mathcal{K}_{H'} = \sum_{j=1}^{\lambda-1}(\sum_{i=1}^{\tau_j} i\varphi_{ji})$. Thereby, Proposition 3 holds. □

C. COMPARISON BETWEEN α_1-NET AND α_2-NET

Finally, we point out that α_1-net and α_2-net do have some common characteristics. Firstly, both of the two kinds of models are subclasses of the α-net. The *conservation law* reported in [1] is not applicable to these $\mathcal{H}^s(r)$-contained models, since the initial marking change of their resource places can definitely influence $\mathcal{K}$. For the H-component (H′-component) in α_1-net (α_2-net), $\mathcal{K}_H$ ($\mathcal{K}_{H'}$) varies according to the changes of the initial making of each strongly independent resource place in $\mathcal{H}^s(r)$. In fact, by comparing the optimal steps $\mathcal{K}$ of α_1-net and α_2-net, it can be concluded that for an α-net (N, M_0), its optimal $\mathcal{K}$ depends on not only the structure and the initial marking within the $\mathcal{H}^s(r)$-contained subnet, but also the structure of the $\mathcal{H}^s(r)$-free subnet. Moreover, the expression of $\mathcal{K}$ with respect to α_1-net is similar to the one with α_2-net, which shows the uniformity of these two subnets, i.e., they are α-net essentially.

In summary, for a net with a ξ-resource, we aim to find a relation between $\mathcal{K}$ and the structure as well as the resource configuration, which can be applied to more general models, to avoid deadlocks efficiently. However, for further investigation, the S^{3}PR with more than one ξ-resource is necessary to study. Such cases are introduced in Section IV, where an optimal DAP for a kind of net with two ξ-resources is considered.

IV. A DAP FOR S^{3}PR WITH TWO ξ-RESOURCES

This section analyzes the number of look-ahead steps to obtain a DAP for an S^{3}PR with two ξ-resources. In the previous sections, we present some optimal multi-step look ahead approaches for two kinds of S^{3}PRs with one ξ-resource only. By an algorithm, the bad markings (those in DZ, but not dead markings generated from the considered S^{3}PR) are divided into two parts. The first part contains the markings at which at least a strict minimal siphon of the S^{3}PR model is emptied. Such bad markings can be found directly. The other part of bad markings at which no siphon is emptied can be distinguished as well. On the other hand, for an S^{3}PR without a ξ-resource, there is an algorithm with polynomial complexity to determine the safety of any reachable state. Therefore, an optimal DAP with polynomial complexity is constructed by a one-step look-ahead method [2]. Different models may lead to different optimal DAP as well as the look-ahead steps $\mathcal{K}$.

In this section, the above mentioned system is expanded to the S^{3}PR with two ξ-resources. It can be verified that there do exist both similarity and difference between the S^{3}PRs with one and that with more than one ξ-resource. Meanwhile, a kind of S^{3}PR with two ξ-resources, namely a binary S^{3}PR and its optimal DAP are introduced and analyzed.

We start from an S^{3}PR with two ξ-resources as shown in Fig. 14. Note that we omit the idle places, as discussed before. In this parameterized model, p_{11} and p_{13} are configured to be the two ξ-resources, i.e., $M_0(p_{11}) = M_0(p_{13}) = 1$. More specifically, p_{11} is a ξ-resource shared by RT-circuits $\theta_1 = p_{10}t_{10}p_{11}t_2p_{10}$ and $\theta_2 = p_{11}t_9p_{13}t_4p_{12}t_3p_{11}$. Similarly, p_{13} is a ξ-resource shared by RT-circuits θ_2 and θ_3, i.e., $p_{11}t_9p_{13}t_4p_{12}t_3p_{11}$ and $p_{13}t_8p_{14}t_5p_{13}$. Obviously, θ_2 contains two ξ-resources. Furthermore, as the only parameter,

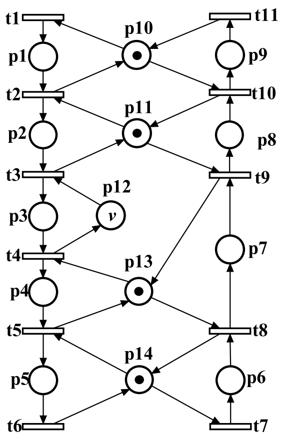

FIGURE 14. A parameterized S^{3}PR model with two ξ-resources.

$M_0(p_{12})$, denoted as v, is supposed to be changed in order to find out the basic rules for calculating $\mathcal{K}$ for this model.

TABLE 8. Simulation results of Fig. 14.

$M_0(p_{12})$	1	2	3	5	10	15	25	50	100	500
$\mathcal{K}$	5	5	5	5	5	5	5	5	5	5

Through the experimental results shown in Table 8, it is easy to find out that $M_0(p_{12})$ does not exert influence on $\mathcal{K}$ for constructing a DAP in this model. Meanwhile, to decipher the relationship between $\mathcal{K}$ and the model structure, it is necessary to deconstruct the structure itself, i.e., study each sub-net of the whole model separately. In Fig. 15, the two deconstructions of the S^{3}PR in Fig. 14, i.e., the two sub-nets B$_1$ and B$_2$, are presented as follows. Each part consists of a ξ-resource and two RT-circuits. Accordingly, $\mathcal{K}$ is divided into two parts which are denoted as $\mathcal{K}_{B_1}$ and $\mathcal{K}_{B_2}$, respectively. For B$_1$ in Fig. 15 (a), p_{11} is the only ξ-resource of the sub-model, and according to the conclusions in [1], it is convenient to compute $\mathcal{K}_{B_1}$ by structural analysis. That is $\mathcal{K}_{B_1} = max\{n+2, p+2\} = max\{2,3\} = 3$. For B$_2$ in Fig. 15 (b), similarly, $\mathcal{K}_{B_2} = max\{n+2, p+2\} = max\{2,2\} = 2$. Note that $\mathcal{K}_{B_1} + \mathcal{K}_{B_2} = 5$, which is exactly $\mathcal{K}$ shown in Table 8. It spontaneously reminds us of the connection between this structure and its optimal DAP.

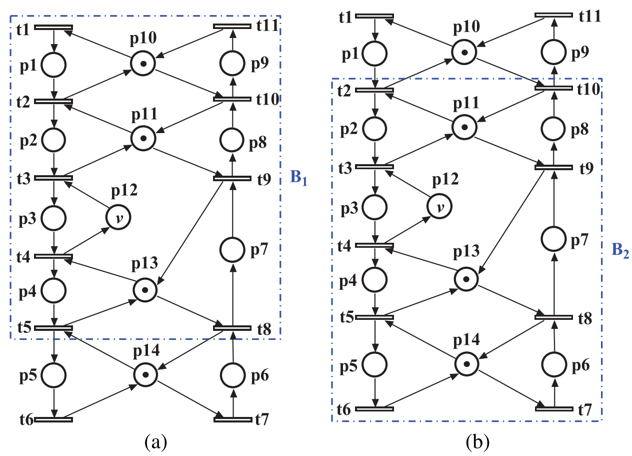

FIGURE 15. Deconstructions of the parameterized S^{3}PR in Fig. 14. (a) Part B$_1$ of the model. (b) Part B$_2$ of the model.

To conclude, as shown in Fig. 15, a subclass of S^{3}PR namely *binary* S^{3}PR (BS^{3}PR) is presented. Furthermore, its optimal DAP is formulated in Proposition 4. The definition of BS^{3}PR is described below.

Definition 14: An S^{3}PR (N, M_0) is said to be binary if there are two ξ-resources r_{ξ_1} and r_{ξ_2} that are intersected by three RT-circuits, i.e., θ_1, θ_2 and θ_3, where $R(\theta_1) \cap R(\theta_2) = \{r_{\xi_1}\}$, $R(\theta_2) \cap R(\theta_3) = \{r_{\xi_2}\}$ and $R(\theta_1) \cap R(\theta_3) = \emptyset$. For all $r \in \mathcal{S}^R_{in}$, $r \in \mathcal{S}^R_{win}$ and for all $r \in P_R \setminus \mathcal{S}^R_{win}$, $M_0(r) = 1$.

Definition 14 presents a fundamental understanding of a binary S^{3}PR. Note that there is no strongly monoploid HR-circuit in a BS^{3}PR, since all independent resources are not strongly independent. Meanwhile, all weakly independent resources belong to a resource-transition circuit and all dependent resources (including two ξ-resources) are initially marked by one.

Now we analyze the model in Fig. 16. There are three RT-circuits, θ_1, θ_2 and θ_3, intersecting with each other in order, and two ξ-resources r_{ξ_1} and r_{ξ_2}. Specifically, $\theta_1 = p_9 t_2 p_{r_{\xi_1}} t_7 p_9$, $\theta_2 = p_{r_{\xi_1}} t_{2n'+1} p_{z_{21}} t_{2n'} \cdots t_{22}$ $p_{z_{2n'}} t_{21} p_{r_{\xi_2}} t_{1m'+1} p_{z_{1m'}} t_{1m'} \cdots t_{12} p_{z_{11}} t_{11} p_{r_{\xi_1}}$ and $\theta_3 = p_{10} t_3 p_{r_{\xi_2}} t_6 p_{10}$. In θ_2, z_{ij} $(i \in \{1, 2\}, j \in \{1, 2, \cdots\})$ represents the arbitrary integer that is assigned to a resource in $\mathcal{S}^R_{win}$ within θ_2 as initial marking parameters. m' and n' represent the numbers of weakly monoploid HR-circuits $(m', n' \in \mathbb{N})$. As shown in Figs. 17 and 18, the model in Fig. 16 is partitioned into two main parts, i.e., B_1 and B_2. To calculate $\mathcal{K}$ for a DAP, we have the following result.

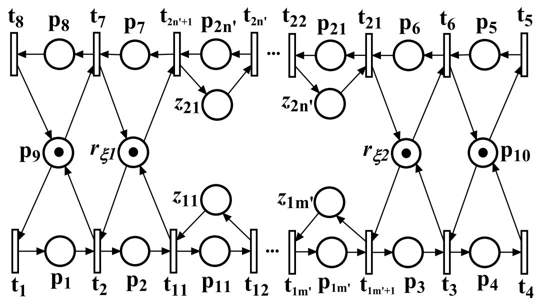

FIGURE 16. A parameterized binary S^3PR.

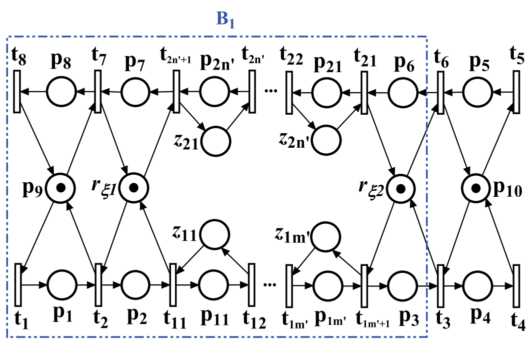

FIGURE 17. Part B_1 of the parameterized binary S^3PR in Fig. 16.

Proposition 4: Given a BS^{3}PR, an optimal DAP $\mathcal{K}$ satisfies

$$\mathcal{K} = m' + n' + 4 \tag{5}$$

Proof: The proof of this proposition is based on the net deconstruction. In a BS^{3}PR, on the one hand, for B_1, according to the conclusions in [1], $\mathcal{K}_{B_1} = max\{2, m' + 2\} = m' + 2$ $(m' \in \mathbb{N})$. Similarly, for B_2, $\mathcal{K}_{B_2} = max\{n' + 2, 2\} = n' + 2$ $(n' \in \mathbb{N})$. To sum up, $\mathcal{K}$ for a BS^{3}PR consists of $\mathcal{K}_{B_1}$ and $\mathcal{K}_{B_2}$, i.e., $\mathcal{K} = \mathcal{K}_{B_1} + \mathcal{K}_{B_2} = m' + 2 + n' + 2 = m' + n' + 4$ $(m', n' \in \mathbb{N})$. □

Note that $m'(n') \geq 0$; therefore, for a BS^{3}PR, $\mathcal{K}_{min} = 4$. In other words, a four-step-look-ahead DAP is the simplest

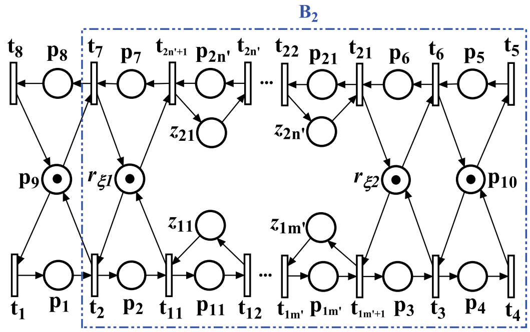

FIGURE 18. Part B_2 of the parameterized binary S^3PR in Fig. 16.

case for this class of S^{3}PR, which contains no weakly monoploid HR-circuit. Last but not the least, this equation shows that all the initial markings of these independent resources in each monoploid $\mathcal{H}(r)$ have no effect on the results, which corresponds to the *conservation law* presented in [1].

V. DISCUSSION

As known, deadlocks in a resource allocation system stem from the improper competition of limited resources. In this paper, resources are categorized into different classes for the computation of the look-ahead steps of an optimal DAP by identifying their roles contributed to an optimal DAP. It is well noted that the existence of a ξ-resource perplexes and exacerbates the design of a deadlock avoidance or prevention policy. Specifically, if there is no ξ-resource in an S^{3}PR, an optimal DAP can be obtained within polynomial time, or an optimal (maximally permissive) liveness-enforcing Petri net supervisor (represented by monitors) can be established by adding a monitor for each strict minimal siphon [2].

However, an interesting result exposed in this paper is that the resources contributed to the steps of an optimal DAP do not contribute to deadlocks. As defined, strongly independent resources are not included in any resource-transition circuit that is a counterpart of siphon causing deadlocks. From the viewpoint of deadlock prevention by computing a set of monitors in an off-line mechanism, they are not shared resources and thus do not contribute to deadlocks. Actually, by Petri net reduction rules proposed in [37] and [48], these resources can be removed from a plant such that the pertinent analysis and computation are significant reduced. In summary, strongly independent resources can be *dropped* when designing a liveness-enforcing supervisor for deadlock prevention; while they cannot be ignored when designing a DAP since they impact to a large extent the number of look-ahead steps. As well-known, if the number of steps to look-ahead is large, the computational cost will increase. That is to say, the computational cost of a DAP is significantly contributed by the resources that do not cause deadlocks. Such a finding motivates us to deliberate upon the strategy of choosing deadlock avoidance and prevention given a system. In this sense, such a finding can be thought of as a substantiation of the power of Petri net theory in the supervisory control of discrete event systems. In the future work, it is necessary to *slim down* an optimal DAP. It is worth of noting that from both perspectives of deadlock avoidance and prevention, the kernel of causing deadlocks is the component containing the ξ-resource, which is the US^{3}PR defined in [1].

VI. CONCLUSION

Based on the considered S^{3}PR models, some structural analysis approaches are proposed in this paper. To achieve the goal of deadlock avoidance, in particular, here the main focus is on structural analysis that does not require the enumeration of the reachability set of a marked net by analyzing the relationship between the structure and the DAP policy. First, a kind of special S^{3}PR models with a ξ-resource, namely α-nets, is presented to expand the results in [1]. Through experiments and simulations, it is formally shown that whether the strongly monoploid HR-circuits are associated with one of the processes or combined as one or several branches of an S^{2}P, their initial marking can inevitably affect $\mathcal{K}$. Then, an S^{3}PR model with two ξ-resources, i.e., BS^{3}PRs, is examined and its multi-step look-ahead-based DAP is proposed. Through the analysis on this kind of models, it is clear that there exists some common characteristics between models with two ξ-resources and those with only one ξ-resource. The research target in future is to apply these methods and results to more general types of Petri net models. We also consider the optimal DAP for a system if there are faults [26], [54]–[56].

ACKNOWLEDGMENT

The authors extend their appreciation to the International Scientific Partnership Program ISPP at King Saud University for funding this research work through ISPP #0079.

REFERENCES

[1] C. Gu, Z. Li, and A. Al-Ahmari, "A multistep look-ahead deadlock avoidance policy for automated manufacturing systems," *Discrete Dyn. Nature Soc.*, vol. 2017, no. 3, pp. 1–16, Aug. 2017, Art. no. 8687035.

[2] K. Xing, M. Zhou, H. Liu, and F. Tian, "Optimal Petri-net-based polynomial-complexity deadlock-avoidance policies for automated manufacturing systems," *IEEE Trans. Syst., Man, Cybern. A, Syst., Humans*, vol. 39, no. 1, pp. 188–199, Jan. 2009.

[3] N. Wu, M. Zhou, and G. Hu, "One-step look-ahead maximally permissive deadlock control of AMS by using Petri nets," *ACM Trans. Embedded Comput. Syst.*, vol. 12, no. 1, pp. 1–23, 2013.

[4] S. Wang, D. You, and C. Seatzu, "A novel approach for constraint transformation in Petri nets with uncontrollable transitions," *IEEE Trans. Syst., Man, Cybern., Syst.*, vol. 48, no. 8, pp. 1403–1410, Aug. 2018, doi: 10.1109/TSMC.2017.2665479.2018.

[5] M. Lawley and S. Reveliotis, "Deadlock avoidance for sequential resource allocation systems: Hard and easy cases," *Int. J. Flexible Manuf. Syst.*, vol. 13, no. 4, pp. 385–404, 2001.

[6] N. Wu, M. Zhou, and Z. Li, "Resource-oriented Petri net for deadlock avoidance in flexible assembly systems," *IEEE Trans. Syst., Man, Cybern. A, Syst., Humans*, vol. 38, no. 1, pp. 56–69, Jan. 2008.

[7] M. Uzam, "An optimal deadlock prevention policy for flexible manufacturing systems using Petri net models with resources and the theory of regions," *Int. J. Adv. Manuf. Technol.*, vol. 19, no. 3, pp. 192–208, Feb. 2002.

[8] J. Ezpeleta, J. M. Colom, and J. Martínez, "A Petri net based deadlock prevention policy for flexible manufacturing systems," *IEEE Trans. Robot. Autom.*, vol. 11, no. 2, pp. 173–184, Apr. 1995.

[9] K. Xing, B. Hu, and H. Chen, "Deadlock avoidance policy for Petri-net modeling of flexible manufacturing systems with shared resources," *IEEE Trans. Autom. Control*, vol. 41, no. 2, pp. 289–295, Feb. 1996.

[10] M. Fanti, "Deadlock resolution strategy for automated manufacturing systems including conjunctive resource service," *IEEE Trans. Syst., Man, Cybern. A, Syst., Humans*, vol. 34, no. 1, pp. 80–92, Jan. 2004.

[11] Z. Li and M. Zhou, *Deadlock Resolution in Automated Manufacturing Systems: A Novel Petri Net Approach*. Glasgow, Scotland: Springer, 2009.

[12] D. You, S. Wang, W. Dai, W. Wu, and Y. Jia, "An approach for enumerating minimal siphons in a subclass of Petri nets," *IEEE Access*, vol. 12, no. 6, pp. 4255–4265, Oct. 2018.

[13] H. Zhang, L. Feng, N. Wu, and Z. Li, "Integration of learning-based testing and supervisory control for requirements conformance of black-box reactive systems," *IEEE Trans. Autom. Sci. Eng.*, vol. 15, no. 1, pp. 2–15, Jan. 2018, doi: 10.1109/TASE.2017.2693995.

[14] Z. Li and M. Zhou, "Elementary siphons of Petri nets and their application to deadlock prevention in flexible manufacturing systems," *IEEE Trans. Syst., Man, Cybern. A, Syst., Humans*, vol. 34, no. 1, pp. 38–51, Jan. 2004.

[15] K. Xing, M. Zhou, F. Wang, H. Liu, and F. Tian, "Resource-transition circuits and siphons for deadlock control of automated manufacturing systems," *IEEE Trans. Syst., Man, Cybern. A, Syst., Humans*, vol. 41, no. 1, pp. 74–84, Jan. 2011.

[16] S. Reveliotis, M. Lawley, and P. Ferreira, "Polynomial-complexity deadlock avoidance policies for sequential resource allocation systems," *IEEE Trans. Autom. Control*, vol. 42, no. 10, pp. 1344–1357, Oct. 1997.

[17] H. Grichi, O. Mosbahi, M. Khalgui, and Z. Li, "RWiN: New methodology for the development of reconfigurable WSN," *IEEE Trans. Autom. Sci. Eng.*, vol. 14, no. 1, pp. 109–125, Jan. 2017.

[18] S. Meskina, N. Doggaz, M. Khalgui, and Z. Li, "Multiagent framework for smart grids recovery," *IEEE Trans. Syst., Man, Cybern., Syst.*, vol. 47, no. 7, pp. 1284–1300, Jul. 2017.

[19] H. Grichi, O. Mosbahi, M. Khalgui, and Z. Li, "New power-oriented methodology for dynamic resizing and mobility of reconfigurable wireless sensor networks," *IEEE Trans. Syst., Man, Cybern., Syst.*, vol. 48, no. 7, pp. 1120–1130, 2018.

[20] M. Gasmi, O. Mosbahi, M. Khalgui, L. Gomes, and Z. Li, "R-Node: New pipelined approach for an effective reconfigurable wireless sensor node," *IEEE Trans. Syst., Man, Cybern., Syst.*, vol. 48, no. 6, pp. 892–905, Jun. 2018.

[21] Z. Li, M. Zhou, and N. Wu, "A survey and comparison of Petri net-based deadlock prevention policies for flexible manufacturing systems," *IEEE Trans. Syst., Man, Cybern. C, Appl. Rev.*, vol. 38, no. 2, pp. 173–188, Mar. 2008.

[22] Z. Li, G. Liu, M. Hanisch, and M. Zhou, "Deadlock prevention based on structure reuse of Petri net supervisors for flexible manufacturing systems," *IEEE Trans. Syst., Man, Cybern. A, Syst., Humans*, vol. 42, no. 1, pp. 178–191, Jan. 2012.

[23] P. Ramadge and W. Wonham, "Supervisory control of a class of discrete event processes," *SIAM J. Control Optim.*, vol. 25, no. 1, pp. 206–230, 1987.

[24] H. Zhang, L. Feng, and Z. Li, "A learning-based synthesis approach to the supremal nonblocking supervisor of discrete-event systems," *IEEE Trans. Autom. Control*, vol. 63, no. 10, pp. 3345–3360, Oct. 2018, doi: 10.1109/TAC.2018.2793662.2018.

[25] P. Ramadge and W. Wonham, "The control of discrete event systems," *Proc. IEEE*, vol. 77, no. 1, pp. 81–89, Jan. 1989.

[26] G. Zhu, Z. Li, N. Wu, and A. Al-Ahmari, "Fault identification of discrete event systems modeled by Petri nets with unobservable transitions," *IEEE Trans. Syst., Man, Cybern., Syst.*, to be published, doi: 10.1109/TSMC.2017.2762823.2018.

[27] K. Barkaoui and I. B. Abdallah, "A deadlock prevention method for a class of FMS," in *Proc. IEEE Int. Conf. Syst., Man Cybern., Intell. Syst. 21st Century*, vol. 5, Oct. 1995, pp. 4119–4124.

[28] K. Barkaoui, A. Chaoui, and B. Zouari, "Supervisory control of discrete event systems based on structure theory of Petri nets," in *Proc. IEEE Int. Conf. Syst., Man, Comput. Cybern. Simulation*, vol. 4, Oct. 1997, pp. 3750–3755.

[29] J. Ye, Z. Li, and A. Giua, "Decentralized supervision of Petri nets with a coordinator," *IEEE Trans. Syst., Man, Cybern., Syst.*, vol. 45, no. 6, pp. 955–966, Jun. 2015.

[30] N. Wu, M. Zhou, and Z. Li, "Short-term scheduling of crude-oil operations: Enhancement of crude-oil operations scheduling using a Petri net-based control-theoretic approach," *IEEE Robot. Autom. Mag.*, vol. 22, no. 2, pp. 64–76, Jun. 2015.

[31] X. Wang, I. Khemaissia, M. Khalgui, Z. Li, O. Mosbahi, and M. Zhou, "Dynamic low-power reconfiguration of real-time systems with periodic and probabilistic tasks," *IEEE Trans. Autom. Sci. Eng.*, vol. 12, no. 1, pp. 258–271, Jan. 2015.

[32] Y. Chen, Z. Li, K. Barkaoui, and A. Giua, "On the enforcement of a class of nonlinear constraints on Petri nets," *Automatica*, vol. 55, pp. 116–124, May 2015.

[33] Y. Chen, Z. Li, K. Barkaoui, N. Wu, and M. Zhou, "Compact supervisory control of discrete event systems by Petri nets with data inhibitor arcs," *IEEE Trans. Syst., Man, Cybern., Syst.*, vol. 47, no. 2, pp. 364–379, Feb. 2017.

[34] L. Bai, N. Wu, Z. Li, and M. Zhou, "Optimal one-wafer cyclic scheduling and buffer space configuration for single-arm multicluster tools with linear topology," *IEEE Trans. Syst., Man, Cybern., Syst.*, vol. 46, no. 10, pp. 1456–1467, Oct. 2016.

[35] N. Wu, M. Zhou, L. Bai, and Z. Li, "Short-term scheduling of crude oil operations in refinery with high-fusion-point oil and two transportation pipelines," *Enterprise Inf. Syst.*, vol. 10, no. 6, pp. 581–610, 2016.

[36] Y. Tong, Z. Li, and A. Giua, "On the equivalence of observation structures for Petri net generators," *IEEE Trans. Autom. Control*, vol. 61, no. 9, pp. 2448–2462, Sep. 2016.

[37] T. Murata, "Petri nets: Properties, analysis and applications," *Proc. IEEE*, vol. 77, no. 4, pp. 541–580, Apr. 1989.

[38] M. Uzam, Z. Li, G. Gelen, and R. S. Zakariyya, "A divide-and-conquer-method for the synthesis of liveness enforcing supervisors for flexible manufacturing systems," *J. Intell. Manuf.*, vol. 27, no. 5, pp. 1111–1129, Oct. 2016.

[39] Y. Chen, Z. Li, A. Al-Ahmari, N. Wu, and T. Qu, "Deadlock recovery for flexible manufacturing systems modeled with Petri nets," *Inf. Sci.*, vol. 381, pp. 290–303, Mar. 2017.

[40] F. Yang, N. Wu, Y. Qiao, M. Zhou, and Z. Li, "Scheduling of single-arm cluster tools for an atomic layer deposition process with residency time constraints," *IEEE Trans. Syst., Man, Cybern., Syst.*, vol. 47, no. 3, pp. 502–516, Mar. 2017.

[41] Y. Hou, N. Wu, M. Zhou, and Z. Li, "Pareto-optimization for scheduling of crude oil operations in refinery via genetic algorithm," *IEEE Trans. Syst., Man, Cybern., Syst.*, vol. 47, no. 3, pp. 517–530, Mar. 2017.

[42] S. Zhang, N. Wu, Z. Li, T. Qu, and C. Li, "Petri net-based approach to short-term scheduling of crude oil operations with less tank requirement," *Inf. Sci.*, vol. 417, pp. 247–261, Nov. 2017.

[43] X. Cong, M. P. Fanti, A. M. Mangini, and Z. Li, "Decentralized diagnosis by Petri nets and integer linear programming," *IEEE Trans. Syst., Man, Cybern., Syst.*, vol. 48, no. 10, pp. 1689–1700, Oct. 2018.

[44] N. Q. Wu and M. C. Zhou, "Schedulability analysis and optimal scheduling of dual-arm cluster tools with residency time constraint and activity time variation," *IEEE Trans. Autom. Sci. Eng.*, vol. 9, no. 1, pp. 203–209, Jan. 2012.

[45] N. Q. Wu and M. C. Zhou, "Modeling, analysis and control of dual-arm cluster tools with residency time constraint and activity time variation based on Petri nets," *IEEE Trans. Autom. Sci. Eng.*, vol. 9, no. 2, pp. 446–454, Apr. 2012.

[46] N. Wu, F. Chu, C. Chu, and M. Zhou, "Petri net modeling and cycle-time analysis of dual-arm cluster tools with wafer revisiting," *IEEE Trans. Syst., Man, Cybern., Syst.*, vol. 43, no. 1, pp. 196–207, Jan. 2013.

[47] H. Liu, J. You, Z. Li, and G. Tian, "Fuzzy Petri nets for knowledge representation and reasoning: A literature review," *Eng. Appl. Artif. Intell.*, vol. 60, pp. 45–56, Apr. 2017.

[48] M. Uzam, "The use of the Petri net reduction approach for an optimal deadlock prevention policy for flexible manufacturing systems," *Int. J. Adv. Manuf. Technol.*, vol. 23, nos. 3–4, pp. 204–219, 2004.

[49] Y. Tong, Z. Li, C. Seatzu, and A. Giua, "Verification of state-based opacity using Petri nets," *IEEE Trans. Autom. Control*, vol. 62, no. 6, pp. 2823–2837, Jun. 2017.

[50] Z. Ma, Z. Li, and A. Giua, "Characterization of admissible marking sets in Petri nets with conflicts and synchronizations," *IEEE Trans. Autom. Control*, vol. 62, no. 3, pp. 1329–1341, Mar. 2017.

[51] Z. Ma, Y. Tong, Z. Li, and A. Giua, "Basis marking representation of Petri net reachability spaces and its application to the reachability problem," *IEEE Trans. Autom. Control*, vol. 62, no. 3, pp. 1078–1093, Mar. 2017.

[52] Y. Hou and K. Barkaoui, "Deadlock analysis and control based on Petri nets: A siphon approach review," *Adv. Mech. Eng.*, vol. 9, no. 5, p. 1687814017693542, 2017.

[53] Y. Hou, Z. W. Li, M. Zhao, and D. Liu, "Extended elementary siphon-based deadlock prevention policy for a class of generalised Petri nets," *Int. J. Comput. Integr. Manuf.*, vol. 27, no. 1, pp. 85–102, 2014.

[54] G. Liu, P. Li, Z. Li, and N. Wu, "Robust deadlock control for automated manufacturing systems with unreliable resources based on Petri net reachability graphs," *IEEE Trans. Syst., Man, Cybern., Syst.*, to be published, doi: 10.1109/TSMC.2018.2815618.2018.

[55] G. Zhu, Z. Li, and N. Wu, "Model-based fault identification of discrete event systems using partially observed Petri nets," *Automatica*, vol. 96, pp. 201–212, Oct. 2018.

[56] X. Wang, Z. Li, and W. Wonham, "Dynamic multiple-period reconfiguration of real-time scheduling based on timed DES supervisory control," *IEEE Trans. Ind. Informat.*, vol. 12, no. 1, pp. 101–111, Feb. 2016.

[57] X. Cong, M. Fanti, A. Mangini, and Z. Li, "On-line verification of current-state opacity by Petri nets and integer linear programming," *Automatica*, vol. 94, pp. 205–213, 2018.

CHAO GU received the B.S. degree in automation from North China Electric Power University, Hebei, China, in 2014, and the M.S. degree in control engineering from Xidian University, Xi'an, China, in 2017.

He is currently pursuing the Ph.D. degree at the School of Electro-Mechanical Engineering, Xidian University. His current research interests include Petri nets, partial observation, and supervisory control of discrete-event systems.

ZHIWU LI (M'06–SM'07–F'16) received the B.S. degree in mechanical engineering, the M.S. degree in automatic control, and the Ph.D. degree in manufacturing engineering from Xidian University, Xian, China, in 1989, 1992, and 1995, respectively. He joined Xidian University in 1992. Over the past decade, he was a Visiting Professor at the University of Toronto, Technion (Israel Institute of Technology), Martin-Luther University, Conservatoire National des Arts et Metiers, Meliksah Universitesi, King Saud University, and the University of Cagliari. He is currently with the Institute of Systems Engineering, Macau University of Science and Technology, Taipa, Macau. His current research interests include Petri net theory and application, supervisory control of discrete event systems, workflow modeling and analysis, system reconfiguration, game theory, and data and process mining. He is a member of the Discrete Event Systems Technical Committee of the IEEE Systems, Man, and Cybernetics Society and a member of the IFAC Technical Committee on Discrete Event and Hybrid Systems from 2011 to 2014. He serves as a frequent reviewer for over 80 international journals, including *Automatica* and a number of the IEEE TRANSACTIONS and many international conferences. He is listed in Marquis Who's Who in the world, 27th Edition, 2010. He was a recipient of an Alexander von Humboldt Research Grant, Alexander von Humboldt Foundation, Germany, and Research in Paris, France. He is the Founding Chair of the Xian Chapter of IEEE Systems, Man, and Cybernetics Society.

NAIQI WU (M'04–SM'04) received the B.S. degree in electrical engineering from the Anhui University of Technology, Huainan, China, in 1982, the M.S. and Ph.D. degrees in systems engineering from Xi'an Jiaotong University, Xi'an, China, in 1985 and 1988, respectively. From 1988 to 1995, he was with the Shenyang Institute of Automation, Chinese Academy of Sciences, Shenyang, China, and from 1995 to 1998 with Shantou University, Shantou, China. He moved to the Guangdong University of Technology, Guangzhou, China, in 1998. He joined the Macau University of Science and Technology, Macau, China, in 2013, where he is currently a Professor at the Institute of Systems Engineering. He has authored or co-authored one book, five book chapters, and over 140 peer-reviewed journal papers. His research interests include production planning and scheduling, manufacturing system modeling and control, discrete event systems, Petri net theory and applications, intelligent transportation systems, and energy systems. He was an Associate Editor of the IEEE Transactions on Systems, Man, and Cybernetics, Part C, the IEEE Transactions on Automation Science and Engineering, the IEEE Transactions on Systems, Man, and Cybernetics: Systems, and an Editor-in-Chief of the *Industrial Engineering Journal*. He is an Associate Editor of *Information Sciences* and the IEEE/CAA Journal of Automatica Sinica.

MOHAMED KHALGUI received the B.S. degree in computer science from Tunis El Manar University, Tunis, Tunisia, in 2001, the M.S. degree in telecommunication and services from Henri Poincaré University, Nancy, France, in 2003, the Ph.D. degree from the National Polytechnic Institute of Lorraine, Nancy, France, in 2007, and the Habilitation Diploma degree in information technology (computer science) from the Martin Luther University of Halle Wittenberg, Halle, Germany, in 2012, with Humboldt Grant. He was a Researcher of computer science with the Institut National de Recherche en Informatique et Automatique INRIA, Rocquencourt, France, ITIA-CNR Institute, Vigevano, Italy, Systems Control Laboratory, Xidian University, Xi'an, China, KACST Institute in KSA, Riyadh, Saudi Arabia, a Collaborator with the SEG Research Group, Patras University, Patras, Greece, the Director of the RECS Project at O3NEIDA, Canada, the Director of the RES Project at Synesis Consortium, Lomazzo, Italy, the Manager of the Cyna-RCS Project at Cynapsys Consortium in France, and the Director of BROS and RWiN Projects at ARDIA Corporation, Germany. He is currently a Professor at Jinan University, China. He has been involved in various international projects and collaborations. He is a member of many TPC of conferences and different boards of journals.

TING QU received the B.S. and M.S. degrees in mechanical engineering from Xi'an Jiaotong University, Xi'an, China in 2001 and 2004, respectively, and the Ph.D. in industrial and manufacturing systems engineering from The University Hong Kong, Hong Kong, China, in 2008. After working as a Post-Doctoral Research Fellow and a Research Assistant Professor with The University Hong Kong and then as a Full Professor at the Guangdong University of Technology, Guangzhou, China, he has been with the School of Electrical and Information Engineering, Jinan University (Zhuhai Campus), Zhuhai, China, since 2016. His research interests include IoT-based smart manufacturing systems and logistics and supply chain management.

ABDULRAHMAN AL-AHMARI received the Ph.D. degree in manufacturing systems engineering from the University of Sheffield, Sheffield, U.K., in 1998. He is currently the Dean of the Advanced Manufacturing Institute and a Professor of industrial engineering with King Saud University, Riyadh, Saudi Arabia. He led a number of funded projects from different organizations in Saudi Arabia. He has published papers in leading *Journal of Industrial and Manufacturing Engineering*. His current research interests include advanced manufacturing technologies, Petri nets, analysis and design of manufacturing systems, computer integrated manufacturing, optimization of manufacturing operations, flexible manufacturing systems and cellular manufacturing systems, and applications of decision support systems in manufacturing.